The CCCH tandem zinc-finger protein Zfp36l2 is crucial for female fertility and early embryonic development

Silvia B. V. Ramos[1], Deborah J. Stumpo[1], Elizabeth A. Kennington[1], Ruth S. Phillips[1], Cheryl B. Bock[2], Fernando Ribeiro-Neto[1] and Perry J. Blackshear[1,3,4,5,*]

[1]Laboratory of Signal Transduction, National Institute of Environmental Health Science, National Institutes of Health, Department of Health and Human Services, Research Triangle Park, NC 27709, USA
[2]Duke Comprehensive Cancer Center, Duke University Medical Center, Durham, NC 27710, USA
[3]The Office of Clinical Research, National Institute of Environmental Health Science, National Institutes of Health, Department of Health and Human Services, Research Triangle Park, NC 27709, USA
[4]Department of Medicine, Duke University Medical Center, Durham, NC 27710, USA
[5]Department of Biochemistry, Duke University Medical Center, Durham, NC 27710, USA
*Author for correspondence (e-mail: black009@niehs.nih.gov)

Accepted 28 June 2004

Development 131, 4883-4893
Published by The Company of Biologists 2004
doi:10.1242/dev.01336

Summary

The CCCH tandem zinc finger protein, Zfp36l2, like its better-known relative tristetraprolin (TTP), can decrease the stability of AU-rich element-containing transcripts in cell transfection studies; however, its physiological importance is unknown. We disrupted *Zfp36l2* in mice, resulting in decreased expression of a truncated protein in which the N-terminal 29 amino acids had been deleted (ΔN-Zfp36l2). Mice derived from different clones of ES cells exhibited complete female infertility, despite evidence from embryo and ovary transplantation experiments that they could gestate and rear wild-type young. ΔN-Zfp36l2 females apparently cycled and ovulated normally, and their ova could be fertilized; however, the embryos did not progress beyond the two-cell stage of development. These mice represent a specific model of disruption of the earliest stages of embryogenesis, implicating Zfp36l2, a probable mRNA-binding and destabilizing protein, in the physiological control of female fertility at the level of early embryonic development. This newly identified biological role for Zfp36l2 may have implications for maternal mRNA turnover in normal embryogenesis, and conceivably could be involved in some cases of unexplained human female infertility.

Key words: Female fertility, Early embryonic development, CCCH tandem zinc-finger proteins

Introduction

Zfp36l2 (Zinc Finger Protein 36 Like 2, also known as TIS11D, ERF2 and BRF2) belongs to an unusual family of zinc finger proteins containing tandem zinc-binding motifs characterized by three cysteines followed by one histidine (CCCH) (Varnum et al., 1991; Blackshear, 2002). Other members of this family in mammals are Zfp36 or tristetraprolin (TTP), also known as TIS11, NUP475 and GOS24 (Lai et al., 1990; Blackshear, 2002); and Zfp36l1 (also known as TIS11B, cMG1, Berg36, ERF1 and BRF1) (Gomperts, 1990; Blackshear, 2002). Through their zinc fingers, these proteins can bind to mRNAs containing class II AU-rich elements (ARE), generally in their 3′-untranslated regions (3′UTR); binding is then followed by degradation of the target mRNAs (Lai et al., 2000).

Increased interest in these proteins came from the phenotype of TTP knockout mice, a systemic inflammatory syndrome that was largely prevented by administration of antibodies to mouse tumor necrosis factor α (TNFα) (Taylor et al., 1996). Macrophages from these mice exhibited increased production of TNFα upon LPS stimulation, because of increased stability of the TNFα mRNA (Carballo et al., 1997). Thus, a model has emerged in which TTP, and possibly its related proteins, bind to the 3′UTR of mRNAs containing class II ARE sequences, resulting in mRNA destabilization and decreased levels of translated proteins (Carballo et al., 1998; Blackshear, 2002).

The zinc finger domains of human ZFP36l2 and ZFP36l1 are 71-73% identical to that of TTP, and they are also able to bind to and destabilize the same set of cytokine mRNAs regulated by TTP (Lai et al., 2000). For example, like TTP, Zfp36l2 can bind to mRNAs containing class II ARE sequences in cell-free and cell transfection experiments, and stimulate their degradation (Lai et al., 2000; Lai et al., 2003); it also shuttles between nucleus and cytoplasm (Phillips et al., 2002). However, virtually nothing is known about its biological function. To gain insights into its physiological role, we disrupted the mouse *Zfp36l2* gene.

Materials and methods

Targeting vector construction

A *Zfp36l2* insertion targeting vector was created by first isolating a *Zfp36l2* clone from a 129SVE mouse genomic library (Stratagene, La Jolla, CA, USA), as previously described (Phillips et al., 2002). The obtained 7.6 kb fragment was then cloned into the *Xba I* site of SK

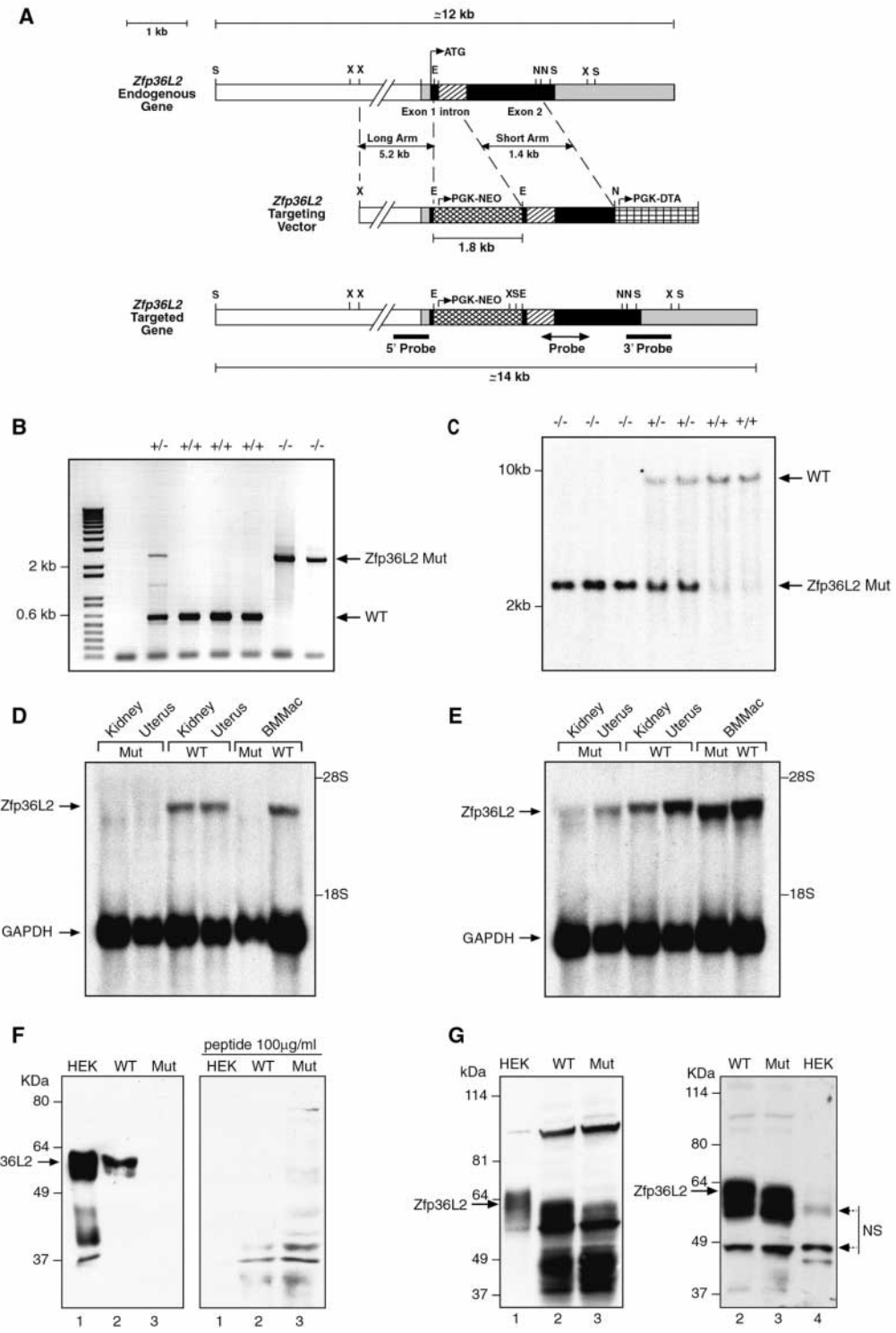

Fig. 1. Generation of the ΔN-Zfp36l2 mutant mouse. (A) The strategy used to disrupt *Zfp36l2* is shown with a schematic representation of the endogenous (12 kb) and targeted (14 kb) alleles of *Zfp36l2*. Restriction sites within the wild-type (WT) and targeted gene (S, *Sst I*; X, *Xba I*; E, *Eco RV*; and N, *Not I*) are indicated. The various shadings represent, respectively, 5′-flanking region of the gene (white), protein coding sequences (black), 5′-UTR and 3′-UTR of the transcript (gray), intron (diagonal-hatch), and PGK-NEO and PGK-DTA cassettes (cross-hatch). A small double arrow indicates the exon 2 probe used for Southern blot analysis. Black bars indicate the location of the 5′ and 3′ probes used in Southern blot analysis to select heterozygous embryonic stem (ES) cells. Genotyping of DNA derived from the progeny of ΔN-Zfp36l2 heterozygous crosses was performed by PCR and Southern blot analysis. (B) An example of the PCR results, in which the ~0.6 kb and ~2.4 kb fragments correspond to WT and *Zfp36l2* mutant alleles, respectively. (C) Total DNA (10 μg) was digested with *Sst I* and probed with an exon 2 probe; the ~10 kb and 2.5 kb bands correspond to the WT and *Zfp36l2* mutant alleles, respectively. (D,E) Total RNA was isolated from the indicated tissues and bone marrow-derived macrophages (BMMac) of WT and mutant (Mut) mice and subjected to northern blot analysis. Each lane in D contains 10 μg of total RNA probed with *Zfp36l2* exon 1 and *Gapd* probes, as indicated by the arrows. The positions of the 28S and 18S ribosomal RNAs are indicated. (E) RNA samples from the same tissues as described in D were subjected to northern blot analysis and hybridized with *Zfp36l2* exon 2 (upper arrow) and *Gapd* (lower arrow) probes, showing the presence of a remaining *Zfp36l2* transcript in the mutant mice. (F) Protein extracts from HEK 293 cells overexpressing Zfp36l2 (lane 1), and bone marrow-derived macrophages from WT and ΔN-Zfp36l2 mutant mice (lane 2 and 3, respectively), were separated on a 10% SDS-PAGE gel and transferred to a nitrocellulose membrane. Blotting with the Zfp36l2 amino-terminal peptide antibody revealed a broad band of ~60 kDa corresponding to the predicted size of Zfp36l2 in the protein extracts from HEK 293 cells overexpressing Zfp36l2 and the cells from the WT mice, but not from the mutant cells (left panel). In the presence of competing peptide, the Zfp36l2 signal was blocked (right panel). (G) Western blot analysis using protein extracts from spleen (left) and BMMac (right) of WT and ΔN-Zfp36l2 mutant (Mut) mice (lane 2 and 3, respectively) and HEK 293 cells overexpressing Zfp36l2-HA (left panel, lane 1) or not expressing Zfp36l2 (right panel, lane 4) were probed with a carboxyl-terminal peptide antiserum. This revealed that the band corresponding to Zfp36l2 exhibited a smaller size in tissues and cells from the mutant mice (arrow), and that the levels of expression of the protein were lower in the spleen, but approximately equal in BMMac. The dotted arrows point to the major non-specific (NS) bands recognized by this antiserum.

(+) (Stratagene) for later procedures. A 5.2 kb *Xba I-EcoR V* fragment, located at the 5′ end of the gene, was isolated from the *Zfp36l2* genomic clone and blunt-ligated into the *Not I* site of the pPGKneobpAlox2PGKDTA vector, generously provided by P. Soriano (Fred Hutchinson Cancer Research Center, Seattle, WA, USA), upstream of the PGK-NEO cassette, encoding the neomycin sequence. The 1.4 kb *EcoR V-Not I* fragment was isolated from the original *Zfp36l2* genomic clone and *Hind III* linkers were added, allowing subsequent ligation to the *Hind III* site of the pPGKneobpAlox2PGKDTA vector, downstream of the 1.8 kb of the PGK-NEO cassette and upstream of the negative selection sequence, PGK-DTA, encoding the diphtheria toxin antigen. The final targeting vector, consisting of 5.2 kb and 1.4 kb fragments corresponding to the long and short homologous arms (Fig. 1A) of *Zfp36l2*, with a 1.8 kb *Neo* fragment interrupting exon 1, 30 bp downstream from the initiator ATG, was linearized with *Kpn I* and electroporated into R1 embryonic stem (ES) cells (Martin, 1981).

Generation of *Zfp36l2*$^{+/-}$ ES cells and chimeric mice

To screen ES cell clones carrying the targeted vector, 10 ng of genomic DNA was used as a template in a single PCR reaction. Eighteen heterozygous ES cell clones were selected by PCR, expanded, and homologous recombination was confirmed by Southern blot analysis. Two ES cell clones with homologous recombination confirmed by Southern (2C11 and 2C12) were separately injected into mouse blastocysts, generating two independent chimeric mouse lines that transmitted a mutant copy of the *Zfp36l2* gene through the germ line.

PCR, Southern, northern and western blot analysis

To genotype the animals, 100 ng of genomic DNA from tails was used as a template in a single PCR reaction containing a forward primer (5′-caggaccccagaaaaatgtcg) and a reverse primer (5′-gttcagattgaggtttgccaggg), resulting in an amplified fragment of ~600 bp in the wild-type (WT) and ~2.4 kb in the Zfp36l2 mutant animals, reflecting the insertion of the *Neo* sequence in that region (Fig. 1B). To confirm the mouse genotyping, Southern blot analysis was performed using 10 μg of genomic DNA digested overnight with *Sst I*. The digested products were loaded into a 0.4% agarose gel and transferred to a nylon membrane. The membrane was UV-crosslinked and probed with a *Zfp36l2* exon 2 ^{32}P random-labeled probe (Fig. 1C).

Primary cells or tissues isolated from mice were used as a source of mRNA. The cells were directly disrupted into a lysis buffer, whereas the dissected tissues were rapidly frozen and pulverized in liquid nitrogen, and processed using the RNeasy kit from Qiagen (Valencia, CA, USA) to extract total cellular RNA. Cytoplasmic RNA from bone marrow-derived macrophages [grown as described in Carballo et al. (Carballo et al., 1997)] was extracted using the same kit, except that the nuclei were removed using a RLN lysis buffer [50 mM Tris-HCl, pH 8, 140 mM NaCl, 1.5 mM $MgCl_2$, 0.5% (v/v) Nonidet P40], according to the directions of the manufacturer. RNA samples (10 μg) were separated by electrophoresis on 1.2% agarose/formaldehyde gels and used for northern blot analysis (Stumpo et al., 1989) with different mouse *Zfp36l2* ^{32}P-labeled probes as described in the figure legends.

Western blot analysis was performed using protein extracts containing overexpressed and endogenous Zfp36l2. For the protein extracts containing overexpressed Zfp36l2, HEK 293 cells were transiently transfected with the mouse full-length *Zfp36l2* cDNA (Phillips et al., 2002) using calcium-phosphate precipitation as described previously (Lai et al., 1999). Protein extracts containing endogenous Zfp36l2 were extracted from bone marrow-derived macrophages, spleen or ovaries, in a lysis buffer composed of β-glycerolphosphate (50 mM, pH 8.2), 0.25 mM sucrose, 1 mM EDTA, 1 mM EGTA, 1 mM dithiothreitol (DTT), 50 mM NaF, 10 mM benzamide-HCl, 0.5 mM phenylmethylsulphonyl fluoride (PMSF), 2 μM peptstatin and 2 μg/ml leupeptin. Ten to 400 μg of protein from a cytosolic fraction of these homogenates was boiled in sample buffer and separated by sodium dodecyl sulphate-polyacrylamide gel electrophoresis (SDS-PAGE). Western blot analysis was performed with antisera directed against either the amino-terminal or carboxyl-terminal peptide of mouse Zfp36l2 (S.B.V.R. and P.J.B., unpublished). The secondary antibody, a goat anti-rabbit polyclonal antibody conjugated with horseradish peroxidase (Bio-Rad Laboratories, Hercules, CA, USA) was diluted to 1:50,000, and proteins were visualized with enhanced chemiluminescence (SuperSignal West Pico, Pierce, Rockford, IL, USA).

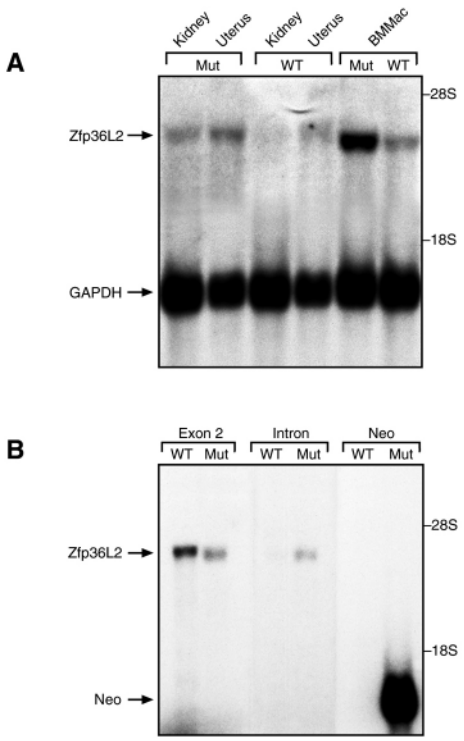

Fig. 2. Presence of sequences from the single intron in the ΔN-Zfp36l2 mutant transcript. (A) Total cellular RNA (10 μg per lane) was isolated from the indicated tissues and bone marrow-derived macrophages (BMMac) of wild-type (WT) and ΔN-Zfp36l2 mutant mice, subjected to northern blot analysis and probed with *Zfp36l2* intron and *Gapd* probes, as indicated by the arrows. (B) Cytosolic RNA was extracted from BMMac of WT and mutant mice, and subjected to northern blot analysis. Each lane contained 10 μg of cytosolic RNA probed, respectively, with *Zfp36l2* exon 2, intron and *Neo* probes, as indicated at the top of each pair of lanes. The new transcript present in cytosolic samples from the mutant mice hybridized with both the exon 2 and intron probes, whereas the WT *Zfp36l2* transcript hybridized only with the exon 2 probe. The new *Zfp36l2* transcript was not fused with *Neo*, because it did not hybridize with a *Neo* probe; as shown in the last lane of this panel, the *Neo* probe hybridized only with the Neo transcript present in the sample from the ΔN-Zfp36l2 mutant cells.

Embryo transfer experiments

WT and *Zfp36l2* mutant females were bred with vasectomized males to induce pseudopregnancy. On day 1.5 post-coitum, WT two-cell stage embryos were transferred into one oviduct of each pseudopregnant female (Brinster et al., 1985).

Ovary transplantation procedure

Young females (4-6 weeks-old) were anesthetized; the left ovary from the recipient animal was removed, and the transplanted ovary (either

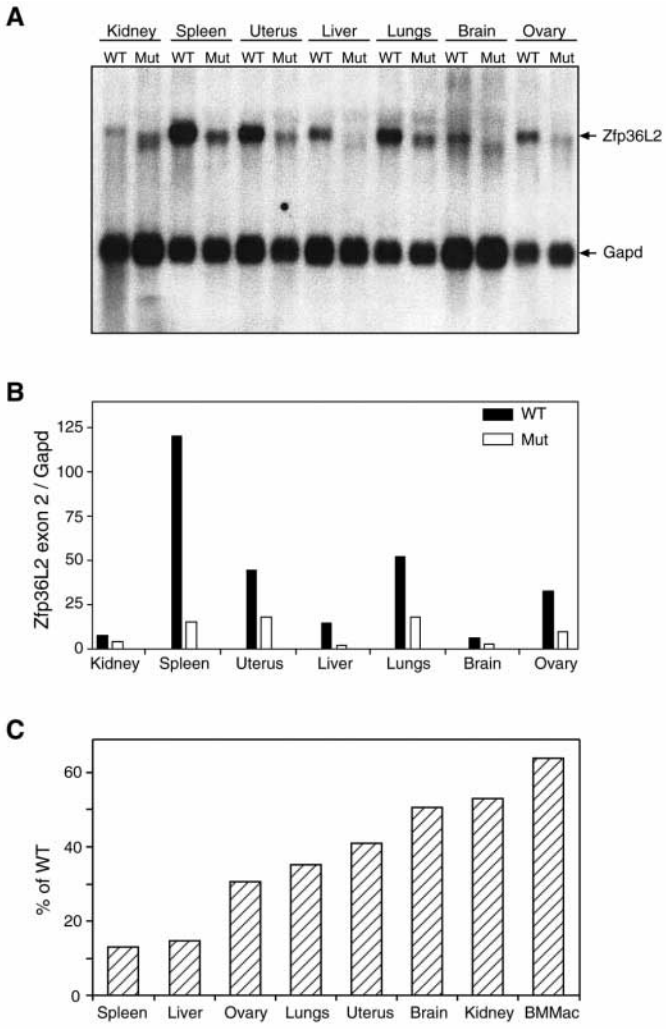

Fig. 3. Expression of *Zfp36l2* transcripts in tissues from mutant mice. (A) Total RNA was extracted from tissues of wild-type (WT) and ΔN-Zfp36l2 mutant mice and subjected to northern blot analysis. Each lane contained 10 μg of total RNA, hybridized with *Zfp36l2* exon 2 and *Gapd* ^{32}P-labeled probes, as indicated by the arrows. Note the decreased size and expression levels of the mutant transcript. (B) The *Zfp36l2* transcripts from the WT and ΔN-Zfp36l2 mutant mice were quantified with a PhosphorImager, and normalized by Gapd mRNA levels. The normalized values were plotted for each tissue. (C) The normalized *Zfp36l2* transcript levels in tissues from the ΔN-Zfp36l2 mutant mice were expressed as percentages of WT transcript levels. The data for bone marrow-derived macrophages (BMMac) were taken from a separate experiment.

+/+ to a –/– recipient, or –/– to a +/+ recipient) was placed inside the previously emptied capsule (Jones and Krohn, 1960). The right ovary was left intact, but its oviduct was cauterized. One week after the surgery, the animals were mated with WT males. Vaginal plugs were checked on a daily basis. Any pups produced were genotyped to confirm that the ova came from the transplanted ovary. Animal care and all experiments were in accordance with institutional guidelines for animal use at NIEHS.

Superovulation, in vivo fertilization and embryo culture

Adult females (5-8 weeks-old) were subjected to exogenous hormone injections to induce superovulation, according to standard procedures (Fraser and Drury, 1975), and then mated with WT males. The next morning, vaginal plugs were checked and in vivo fertilized ova were recovered from the swollen ampulla 17-19 hours after hCG injection. The embryos were briefly treated with hyaluronidase (1 mg/ml) and further cultured in microdrops of Whittens medium (M16) covered with paraffin oil and incubated at 37°C in a humidified atmosphere of 5% CO_2 in air until the time of observation.

Microscopy

For the fluorescent microscopic analysis, the embryos were fixed in 4% (v/v) paraformaldehyde in phosphate-buffered saline (PBS; pH 7.4) for 30 minutes and then stained with 800 nM of Hoechst 33258 dye in a mounting medium composed of PBS azide (25 mg/mL) and 50% glycerol (Perreault and Mattson, 1993). Observation was performed on a Zeiss LSM 510 confocal microscope (Zeiss, Thornwood, NY, USA). The unfixed embryos were photographed using Nomarski optics with 400 ASA black and white film.

DNA probes and accession number

The mouse Zfp36l2 RefSeq currently in GenBank, NP_031591.1, represents a partial protein that lacks the amino terminal contribution of the first exon and is also truncated at the carboxyl-terminal when compared with the current human protein RefSeq NP_008818 (Blackshear et al., 2003). The *Zfp36l2* exon 2 probe corresponds to nucleotides 10176476-10176912 (reverse complement) of the mouse genomic contig represented by GenBank accession number NT_039658.2 and was derived from the EST clone accession number AA021952; this contained approximately 72 bp of unspliced 3′ intron sequence as well as approximately 365 bp of 5′ exon 2 sequence. The *Zfp36l2* exon 1 and intron probes correspond, respectively, to nucleotides 1140-1528 and 1576-2075 of the mouse genomic clone represented by GenBank accession number M97165; the intron probe contained 14 bp of 5′ exon 2 sequence.

Nomenclature

The approved nomenclature for the human gene encoding the third TTP family member is *ZFP36l2* (no OMIM number), whereas the mouse gene is *Zfp36l2*. As mentioned in the text, the encoded protein is also known as TIS11D or 11D, ERF2 and BRF2. Approved gene symbols were obtained from the HUGO Gene Nomenclature Committee and the Mouse Genomic Nomenclature Committee (Blackshear et al., 2003).

Results

Generation of *Zfp36l2* mutant mice expressing a truncated Zfp36l2 protein

The *Zfp36l2* genomic targeting vector was constructed so that the neomycin resistance gene (*Neo*) was inserted into the open reading frame of the *Zfp36l2* first exon (Fig. 1A). This construct was transfected into mouse ES cells, generating several clones containing one copy of the WT gene and one copy of the mutant gene. Two different heterozygous ES cell clones were injected into mouse blastocysts to generate chimeric mice (Koller and Smithies, 1989); these were then crossed with C57BL/6NTac and 129S6/SvEvTac mice, establishing two independent colonies of mice on each genetic background. Homozygous mutant mice (–/–), referred to here as ΔN-Zfp36l2 mice, were identified by a polymerase chain reaction (PCR)-based genotyping assay, performed on the progeny of heterozygous (+/–) matings (Fig. 1B); the genotypes were also confirmed by Southern blot analysis (Fig. 1C). Northern blot analysis revealed that the mutant mice lacked an mRNA hybridizing with a selective *Zfp36l2* exon 1 probe (Fig. 1D). Moreover, western blot analysis with an

antiserum that reacts specifically with the amino-terminus of Zfp36l2, but not with Zfp36l1 or TTP, revealed specific immunoreactivity in cell extracts derived from WT mice but not from mutant mice (Fig. 1F). These data demonstrate that the targeting vector successfully disrupted both copies of the *Zfp36l2* gene at its target site. However, a specific probe for exon 2 demonstrated the presence of a remaining transcript in cells and tissues from the mutant mice (Fig. 1E). In addition, a carboxyl-terminal peptide antibody demonstrated the presence of a truncated version of the Zfp36l2 protein with faster electrophoretic mobility (ΔN-Zfp36l2) in the mutant mice. Expression of ΔN-Zfp36l2 was significantly reduced in protein extracts from tissues of the mutant mice (Fig. 1G, left panel), although it approached WT levels in cultured bone marrow-derived macrophages (Fig. 1G, right panel). These data indicated that the mutant mice expressed reduced levels of an amino-terminal truncated form of Zfp36l2.

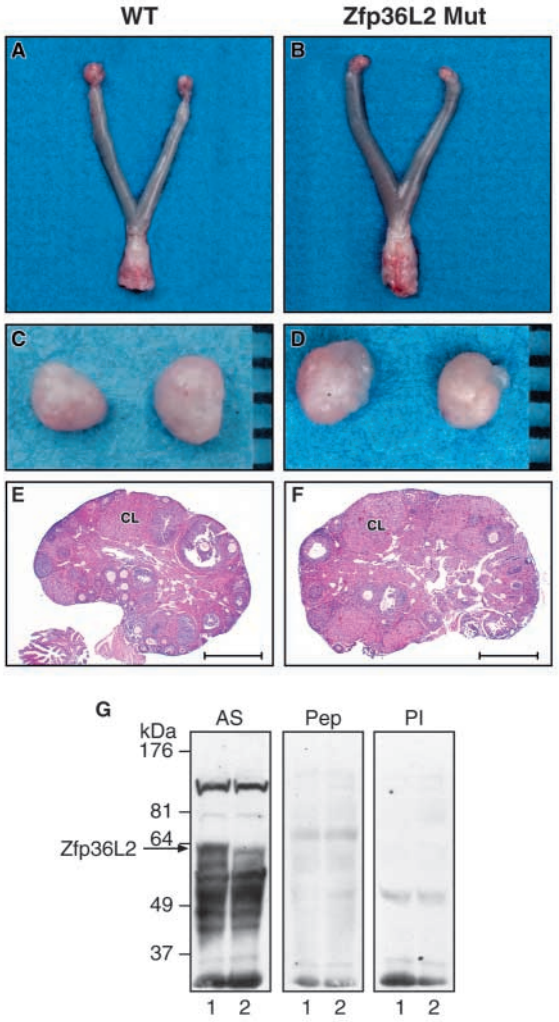

Fig. 4. Anatomy of ΔN-Zfp36l2 mutant female reproductive tract. Ovaries from adult (8-12 weeks old) female mice, synchronized with respect to the ovulatory cycle, were dissected from the fat pad, weighed and then fixed. The top and middle panels show the macroscopic anatomy of the female reproductive tract and the ovaries from wild-type (WT) (A,C) and ΔN-Zfp36l2 mutant mice (B,D). The lower panel shows representative ovary sections stained with hematoxylin and eosin from females in post-estrus. No apparent abnormalities were noted in the ΔN-Zfp36l2 mutant ovaries (F) in comparison with the WT (E); both exhibited follicles at various stages of development, as well as corpora lutea (CL). Scale bars: 1 mm. (G) Western blot analysis was performed using protein extracts from ovaries of WT (lanes 1) and ΔN-Zfp36l2 mutant mice (lanes 2). These were probed with a carboxyl-terminal peptide antiserum (AS) or with pre-immune serum (PI). The band corresponding to the top band of Zfp36l2 was smaller in size in the ovaries from the mutant mice (arrow), and the level of expression of the protein appeared to be decreased in comparison with the WT. The smaller bands probably represent some combination of degraded fragments of Zfp36l2, phosphorylated isoforms, or possibly cross-reaction with the much smaller Zfp36l1 protein. In the presence of competing peptide (middle panel), the AS recognition of the Zfp36l2 band and the smaller bands was blocked.

Expression of the *Zfp36l2* intron in mature transcript from mutant mice

In transcripts from mutant mice, exon 2 appeared to be fused with at least part of the single intron present in *Zfp36l2*, but not with the *Neo* transcript (Fig. 2). Expression of transcripts hybridizing to the *Zfp36l2* intron was markedly increased in total RNA derived from cells and tissues of the ΔN-Zfp36l2 mutant mice as compared with WT (Fig. 2A). Because unprocessed RNA is generally nuclear, we investigated whether the *Zfp36l2* intron was expressed in cytosolic RNA derived from WT and ΔN-Zfp36l2 mice. As shown in Fig. 2B, the *Zfp36l2* intron was not detected in cytosolic RNA preparations from WT mice, but abundant expression was observed in samples from the ΔN-Zfp36l2 mice, demonstrating that at least a portion of the *Zfp36l2* intron is part of the mature transcript present in the mutant mice. Direct sequencing of this new transcript confirmed that 403 bp corresponding to the 3′-end of the intron was fused with the second exon of *Zfp36l2* (not shown). The *Zfp36l2* intron is very rich in GC nucleotides (~70%), which has hampered our efforts to sequence the extreme 5′-end of the mutant transcript.

Decreased expression of *Zfp36l2* exon 2 in transcripts from mutant mice

The ΔN-Zfp36l2 mutant transcript appeared to be approximately 400 bp smaller than the WT transcript (Fig. 2B). Transcripts with increased mobility were also observed in several tissues from the mutant mice (Fig. 3A). Moreover, the expression levels of the mutant transcript containing the exon 2 of *Zfp36l2* were decreased to various degrees in tissues from the ΔN-Zfp36l2 mice (Fig. 3B). Spleen, liver and ovary expressed only 12, 15 and 30 percent of WT values, respectively (Fig. 3C), whereas cultured bone marrow-derived macrophages exhibited the closest to normal levels of transcript hybridizing with the exon 2 probe (approximately 65% of the WT values) (Fig. 1E, Fig. 3C); they also expressed ΔN-Zfp36l2 protein at levels approaching those seen in the WT cells (Fig. 1G).

These data demonstrated that tissues from the mutant mice expressed decreased levels of the mutant exon 2-containing transcript, presumably leading to decreased expression of an amino-terminal truncated form of Zfp36l2 (Fig. 1G, left panel). This truncated protein is likely to be translated from the only remaining methionine in frame with the rest of the protein encoded by exon 2 (analogous to methionine 29 in the human GenBank RefSeq NP_008818). The predicted size of the

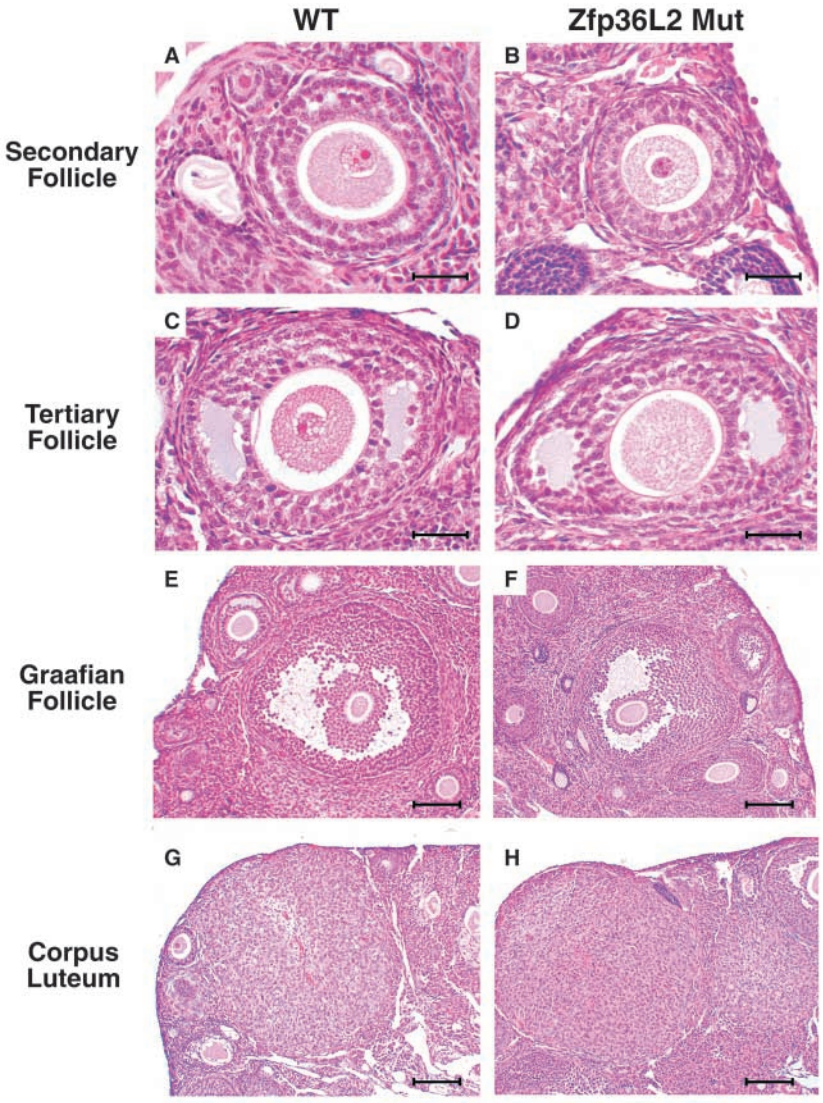

Fig. 5. Ovary and oocyte morphology in adult wild-type (WT) and ΔN-Zfp36l2 mutant females. (A,B) Secondary follicles in which the small oocytes are surrounded by cuboidal cells. (C,D) Tertiary follicles are shown in which the cuboidal cells have divided actively, forming a stratified layer around the oocyte. Irregular spaces have appeared, forming the follicular antrum. (E,F) Graafian follicles, in which the large follicular cavity is distended with fluid, and the cumulus oophorus contains a mature oocyte surrounded by a thick zona pelucida and well-formed corona radiata. (G,H) The corpora lutea, which appear to form normally after ovulation. Scale bars: 40 μm in A-D; 100 μm in E-H.

truncated protein is ~3 kDa smaller than the WT, corresponding to the size difference observed in western blot analysis (Fig. 1G). The mouse RefSeq for this protein (NP_031591.1) does not yet reflect the full-length protein sequence, but the antibody evidence presented here firmly establishes that the normal mouse protein contains an amino-terminal extension contributed by exon 1.

To date, biochemical assays with the WT and ΔN-Zfp36l2 proteins expressed in 293 cells have shown no differences in three assays of tandem CCCH zinc finger protein function: binding to ARE-containing RNA probes in a gel shift assay; deadenylation of a modified TNF transcript in cell-based co-transfection assays (Lai et al., 1999); and stimulated deadenylation of ARE-containing, polyadenylated RNA probes in a cell-free assay (Lai et al., 2003) (S.B.V.R., W. S. Lai and P.J.B., unpublished). In addition, the cytosolic localizations of ΔN-Zfp36l2-GFP and WT-Zfp36l2-GFP expressed in 293 cells were indistinguishable (S.B.V.R. and P.J.B., unpublished).

Homozygous ΔN-Zfp36l2 females are sterile despite normal estrous cycles and sexual behavior

Heterozygous matings from two independent mouse colonies on the C57BL/6NTac background generated 305 offspring, with genotypes of 79 (26%) WT, 153 (50%) heterozygous, and 73 (24%) *ΔN-Zfp36l2*$^{-/-}$ homozygous. The percentages of males (27:49:24) and females (24:51:24) of each genotype followed the same distribution. This typical Mendelian inheritance pattern indicated that the targeted disruption of the open reading frame of the *Zfp36l2* gene at exon 1 had no deleterious effect on viability when both eggs and sperm came from heterozygous animals. The ΔN-Zfp36l2 mice exhibited apparently normal lifespans. In contrast to the TTP-deficient mice (Taylor et al., 1996; Carballo et al., 1998), no evidence of systemic inflammation has been detected under normal husbandry conditions, and macrophages from ΔN-Zfp36l2 mice express similar levels of TNFα mRNA as the WT cells when exposed to LPS (not shown). The observed Mendelian frequency of ΔN-Zfp36l2 mice is also in contrast to mice deficient in another family member, Zfp36l1, which die in mid gestation (Stumpo et al., 2004).

The only observed phenotype in the homozygous ΔN-Zfp36l2 females was complete infertility, whereas the males were fertile. This was observed in two independent mouse colonies derived from distinct ES cell clones, through seven backcrosses into the C57BL/6NTac strain; it was also seen in the 129S6/SvEvTac background, in mouse colonies derived from both ES cell clones. These data strongly suggest that the female infertility phenotype was caused by the disruption of *Zfp36l2*.

To gain insights into the etiology of this infertility, ΔN-Zfp36l2 female mice were subjected to a continuous mating study with stud males for six months, and evaluated for cycling, behavioral estrous and mating. The ΔN-Zfp36l2 female mice (n=14) bred on multiple occasions, as determined by the presence of vaginal plugs every 5-6 days; however, no pregnancies were observed. This cyclical presence of vaginal plugs suggested that the mutant females exhibited typical estrous cycles and normal sexual behavior. The anatomy of their reproductive tracts also appeared normal (Fig. 4A-F), even though their ovaries expressed ΔN-Zfp36l2 protein at lower levels

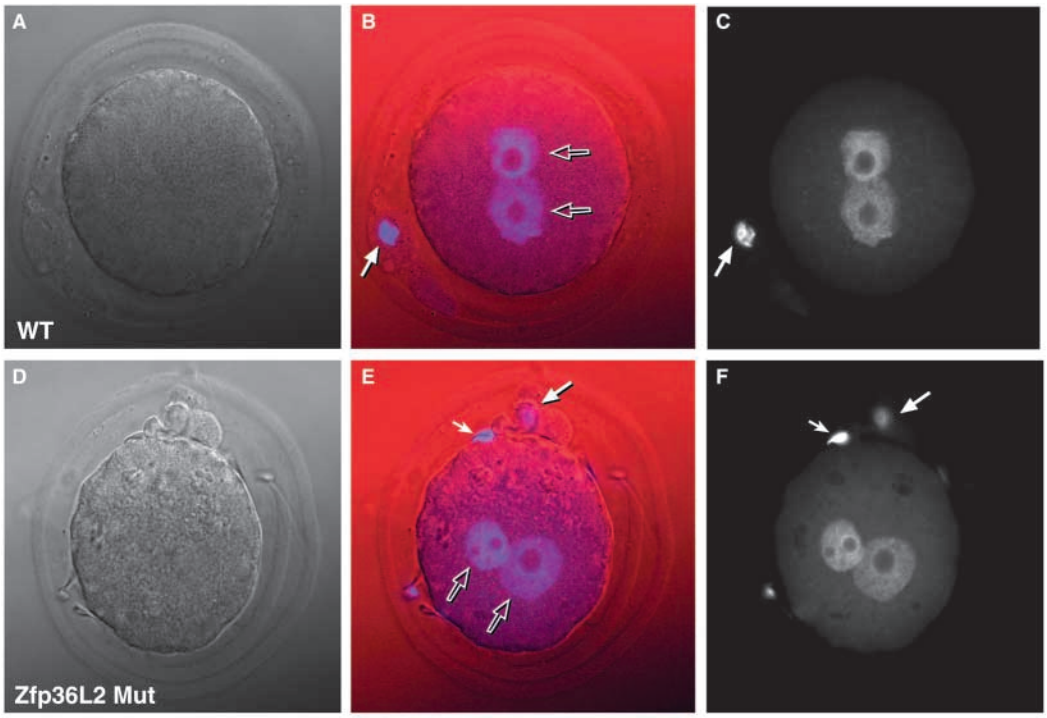

Fig. 6. Fertilization of ova in ΔN-Zfp36l2 mice. Ova from wild-type (WT) (A-C, upper panels) and ΔN-Zfp36l2 mutant females (D-F, lower panels) were collected from the oviduct 8-10 hours after in vivo fertilization of superovulated females, kept in culture for 4-5 hours, then fixed and stained with a chromosome dye (Hoechst 33258) and analyzed by confocal microscopy. These images are representative of three separate experiments. (A,D) Differential interference contrast images show apparently normal morphology, in which both ova are surrounded by zona pelucida. Chromosome staining of the same cells (C,F) demonstrated that ova from both the WT and ΔN-Zfp36l2 mutant females showed typical markers of fertilization, such as the presence of two pronuclei and the formation of a second polar body (large filled arrow). A supernumerary sperm is indicated by the filled small arrow in E,F. In the middle panels (B,E), the left and right images were superimposed showing the localization of the second polar bodies (large filled arrows) and the two pronuclei (large open arrows) in relation to the surrounding zona pelucida, as well as the supernumerary sperm in E (small filled arrows).

than the full-length Zfp36l2 in WT mice (Fig. 4G). Thus, homozygosity for *ΔN-Zfp36l2* had no obvious deleterious effects on the development of the female reproductive tract.

ΔN-Zfp36l2 mutant female can carry full-term pregnancies upon WT embryo transfer

We investigated a possible uterine origin for the infertility with embryo transfer experiments (Brinster et al., 1985). For this, pseudopregnancies were induced in ΔN-Zfp36l2 females followed by the transfer of WT embryos into the mutant animals. Two of five homozygous mutant females successfully transplanted with WT embryos became pregnant, delivered viable litters, lactated, and nurtured their pups to weaning age. Similarly, two out of four WT females carried successful pregnancies after transplantation of WT embryos. Thus, the ΔN-Zfp36l2 females were hormonally competent to carry a pregnancy to full term, and exhibited normal labor and maternal behavior. These findings excluded uterine and corpus luteum defects, as well as hypothalamic-pituitary dysfunction, as the cause of the female infertility seen in the ΔN-Zfp36l2 animals.

Rescue of ΔN-Zfp36l2 female sterility by transplantation of WT ovaries

A potential ovarian etiology for the infertility of the ΔN-Zfp36l2 females was investigated by classical ovary transplant experiments (Jones and Krohn, 1960). Donor ovaries from ΔN-Zfp36l2 animals were transplanted into WT females, from which the left ovary had been removed, leaving the right ovary in situ but with a cauterized oviduct. Although all five WT females transplanted with ΔN-Zfp36l2 ovaries displayed copulatory plugs, none carried a successful pregnancy (Table 1). In contrast, three out of five ΔN-Zfp36l2 females transplanted with WT ovaries carried successful pregnancies; that the offspring were derived from WT oocytes was confirmed by genotyping. Transplantation of WT ovaries into heterozygous females, known to have no fertility defect, showed a similar rate of successful pregnancies (68%), reflecting the efficacy of the surgical procedure.

ΔN-Zfp36l2 females ovulate naturally and in response to exogenous hormone treatment

These findings suggested that the infertility of the ΔN-Zfp36l2 females was because of ovarian and/or an oocyte dysfunction.

Table 1. Transplantation of ovaries from ΔN-Zfp36L2 mice into wild-type females

Recipient	Donor	Plugs	Pregnancy	Pups
Wild type (*n*=5)	ΔN-Zfp36L2	+	0/5	º
ΔN-Zfp36L2 (*n*=5)	Wild type	+	3/5	WT
Het* (*n*=6)	Wild type	+	4/6	WT

Het*, heterozygous

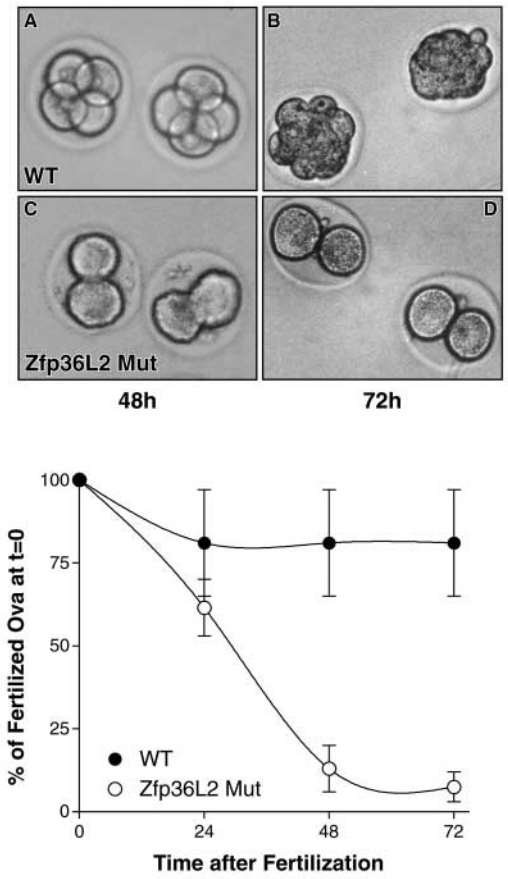

Fig. 7. Arrest of embryos from ΔN-Zfp36l2 females at the two-cell stage. Wild-type (WT) and ΔN-Zfp36l2 mutant females were superovulated and mated with WT stud males. Nineteen hours after the hCG injection, all potential in vivo fertilized ova were collected and incubated in M16 growth medium. After 5 hours in culture, the fertilized ova were sorted based on the morphological detection of two pronuclei and the presence of a second polar body, thus considered time zero for the fertilization. The unfixed embryos were photographed at 50× using Nomarski optics. The upper panel illustrates the normal development of embryos from WT females after 48 hours (A) and 72 hours (B) in culture; the embryos derived from ΔN-Zfp36l2 mutant females at equivalent incubation periods are shown in C,D. The graph represents means ±s.d. results from three such experiments, in which the means of the numbers of actively dividing embryos derived from WT (black circles) and ΔN-Zfp36l2 mutant females (white circles) were significantly different at 48 and 72 hours ($P<0.01$, using Student's *t*-test), but not at 24 hours.

However, mutant and WT ovaries from age-matched females had similar weights: WT, 4.5 mg±0.3 mg (mean±s.d.), $n=9$; ΔN-Zfp36l2, 4.2 mg±0.2 mg, $n=7$; $P>0.10$, using Student's *t*-test. In addition, ovaries from adult (8-12 weeks old) ΔN-Zfp36l2 females exhibited no apparent anatomical or histological abnormalities (Fig. 4D,F). Follicles were present at all developmental stages, ranging from primordial to fully developed follicles with a defined antrum (Fig. 4F, Fig. 5B,D,F,H). These findings tend to rule out a gross defect in the development of ovarian follicular structures, or in the maturation of ΔN-Zfp36l2 oocytes.

ΔN-Zfp36l2 females could ovulate naturally, as suggested by the presence of corpus lutea in the ovaries of these animals, indicating past spontaneous ovulations (Fig. 4F, Fig. 5H). The ovarian responsiveness to exogenous hormonal treatment was also evaluated. For this, age-matched (5-8 weeks old) mutant and WT littermate females were primed with hormones according to a standard superovulation protocol (Fraser and Drury, 1975) and allowed to mate with stud males. Whereas the ΔN-Zfp36l2 and WT females displayed indistinguishable copulatory efficiency, the ΔN-Zfp36l2 females released approximately 60% as many ova as the WT; for example, in one representative experiment, 100 ova were recovered from ΔN-Zfp36l2 females ($n=9$) versus 170 ova from WT mice ($n=9$). This suggested that the infertility observed in the ΔN-Zfp36l2 females might, at least in part, be related to a dysfunction in hormone-induced ovulation. However, the mutant ova released after hormone treatment were morphologically indistinguishable from the WT cells. Differential interference contrast imaging showed that the size, shape and general appearance of the mutant ova were comparable to those originating from WT females (Fig. 6A,D), consistent with the findings from ovarian histological analysis. The substantial rate of ovulation observed in the ΔN-Zfp36l2 females upon hormonal stimulation indicates that their ova had accomplished the first meiotic division. This suggests that the ΔN-Zfp36l2 protein does not have a major deleterious effect on the hormone-regulated processes responsible for overcoming the meiotic arrest. Thus, it seems unlikely that abnormal oocyte maturation and/or hormone-induced ovulation were responsible for the complete infertility phenotype of the ΔN-Zfp36l2 females.

ΔN-Zfp36l2 ova can be fertilized but the embryos do not develop beyond the two-cell stage

We next evaluated the possibility that a fertilization defect was related to the sterility of the ΔN-Zfp36l2 females. We observed that the ova from the mutant females could be fertilized in vivo, as shown by the presence of two pronuclei and the formation of a second polar body (Fig. 6E,F), both diagnostic features of fertilization. These findings indicated that the ova from ΔN-Zfp36l2 females could overcome the meiotic metaphase II arrest and successfully accomplish the second meiosis, a phenomenon triggered by fertilization. We then investigated the pre-implantation development in culture of ova fertilized in vivo in ΔN-Zfp36l2 females. The embryos derived from the ΔN-Zfp36l2 females crossed with WT males were able to undergo the initial cleavage step, indicating that the mutant protein did not prevent the first mitotic division of the embryo. However, although the WT embryos progressed to the four-cell and morula stages after 48 and 72 hours in culture, respectively (Fig. 7A,B), the embryos derived from ΔN-Zfp36l2 mutant females remained arrested at the two-cell stage (Fig. 7C,D). We conclude that this blockage of early embryonic development at the two-cell stage is causally linked to the infertility seen in the ΔN-Zfp36l2 females.

Discussion

These results implicate the ΔN-Zfp36l2 protein in the control of early embryonic development, specifically in the progression of the embryo beyond the two-cell stage. Among previous genetically engineered mouse models of female infertility (Matzuk and Lamb, 2002), to our knowledge the

specific phenotype of a two-cell stage block is analogous only to the disruption of *Mater* (Fig. 8); this phenotype is thought to be because of decreased embryonic transcription (Tong et al., 2000). The ΔN-Zfp36l2 females therefore provide evidence for a critical role of this presumed mRNA destabilizing protein in the regulation of early embryonic development.

The ΔN-Zfp36l2 mice exhibited a dual defect: absence of the amino terminal 29 amino acids of mouse Zfp36l2, which are contributed by the first exon and part of the second; and decreased levels of this truncated protein, with the extent of the decrease varying among tissues. It seems unlikely that ΔN-Zfp36l2 functions as a dominant-negative mutant, i.e. interfering with the action of WT Zfp36l2, because the WT Zfp36l2 protein is not expressed in the mutant females. However, we cannot completely exclude the possibility that ΔN-Zfp36l2 behaves as a dominant-negative inhibitor of the WT protein shortly after fertilization and during co-expression of the ΔN-Zfp36l2 and WT Zfp36l2 proteins in the very early embryo; this would occur, for example, after a mating between a mutant female and a WT male. Arguing against this possibility is that the reproductive success rate of the ΔN-Zfp36l2 heterozygous females was indistinguishable from that of the WT females. In addition, the function of the ΔN-Zfp36l2 protein was essentially identical to that of the WT protein in three different assays of tandem CCCH zinc finger protein function. Therefore, we think that it is most likely that *ΔN-Zfp36l2* represents a partial loss-of-function mutation, pointing to an unidentified critical role of Zfp36l2 in the maternal control of early embryo development.

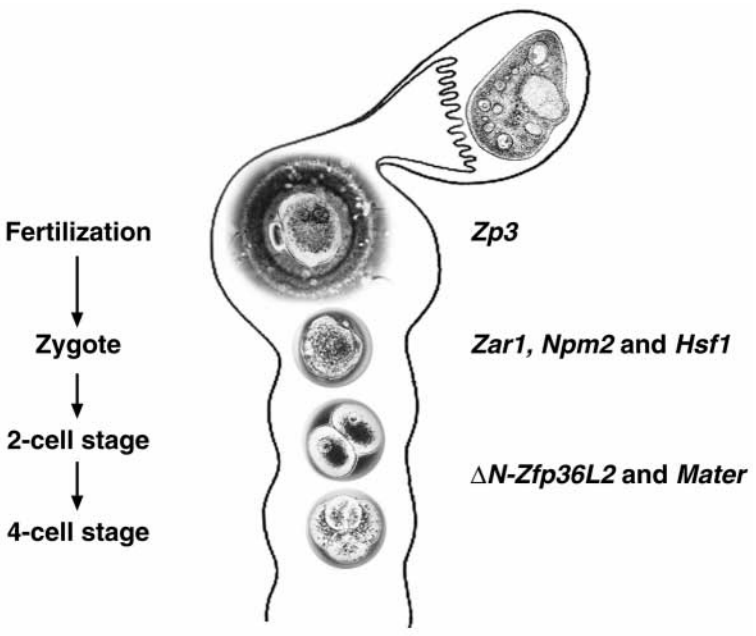

Fig. 8. Genetic models of mouse female infertility because of blockage of early embryonic development. The left column specifies the stage of development along the oviduct. The right column lists the genes associated with blockage at each stage. The zona pelucida protein Zp3 has been implicated in impaired fertilization (Liu et al., 1996; Rankin et al., 1996). Disruption of *Npm2* (Burns et al., 2003), *Zar1* (Wu et al., 2003) and *Hsf1* (Christians et al., 2000) impedes the first cleavage step. Blockage at the two-cell stage is observed with disruption of *Zfp36l2 (ΔN-Zfp36l2*) and *MATER* (Tong et al., 2000).

As noted in the Results section, two lines of mice derived from distinct ES cell clones, each in two distinct genetic backgrounds, C57BL/6NTac and 129S6/SvEvTac, exhibited complete female infertility as the only apparent phenotype. This was in the setting of apparently normal female reproductive behavior, reproductive tract anatomy, uterine function and maternal behavior, and the ability of the ovary to release oocytes and form corpus lutea. Ova derived from the ΔN-Zfp36l2 females could also be fertilized, but the zygotes then divided only once and ceased cell division. There was also a modest decrease in the number of oocytes released after superovulation, suggesting the possibility of an abnormal ovarian environment for oocyte maturation and/or release.

The physiological function of TTP, the prototype of this family of CCCH tandem zinc finger proteins, is to destabilize certain ARE-containing mRNAs, of which GM-CSF and TNF are known to be affected in cells derived from TTP knockout mice (Blackshear, 2002). In early development, degradation of maternal mRNAs is coupled to activation of transcription by the newly formed zygotic nucleus (zygotic gene activation) (Bachvarova and De Leon, 1980; Clegg and Pikó, 1983; Schultz, 1993). It seems possible that Zfp36l2 could mediate the destabilization of specific maternal transcripts in early embryonic development. In the mouse, the initiation of zygotic gene activation occurs at the transition from the initial cleavage step to the two-cell stage. This process has been linked to a massive degradation of maternal mRNAs – remarkably, approximately 40% of the maternal RNA pool is lost during embryo development from the one- to two-cell stage (Bachvarova and De Leon, 1980), by mechanisms that are presently unknown.

Translational activation of masked maternal transcripts by addition of a long poly(A) tail is also an important regulatory process triggered by fertilization that is required for early embryonic development (Wormington, 1994). Because TTP and its family members can promote the deadenylation of ARE-containing mRNAs (Lai et al., 1999), it is possible that a putative deadenylation function of ΔN-Zfp36l2 may also affect the translation of proteins required for early embryonic development.

After fertilization, the initial developmental program implements the degradation of maternal proteins and maternal mRNAs. Studies in *C. elegans* have shown that some invertebrate CCCH zinc finger proteins such as PIE-1, POS-1, MEX-1, MEX-5 and MEX-6 are important for proper execution of developmental programs (Mello et al., 1996; Tabara et al., 1999; Guedes and Priess, 1997; Schubert et al., 2000). In these models, the asymmetric segregation of CCCH proteins between germ and somatic cells is important for the formation of the so-called germ plasma and depends on the degradation of CCCH proteins in somatic cells (DeRenzo et al., 2003). OMA-1 and OMA-2 have been likened to mammalian TTP-like proteins; whereas single knockouts of their genes have no phenotype in *C. elegans*, disruption of both leads to impairment of oocyte maturation and female infertility

(Detwiler et al., 2001). Interestingly, a single point mutation in OMA-1 (*zu405*) leads to an embryonic lethal phenotype because of increased stability of the mutant protein (Lin, 2003).

Although most of the *C. elegans* CCCH proteins do not exhibit the spacing and other requirements that define the TTP family of tandem CCCH zinc finger proteins in mammals, the amino acids that coordinate zinc are identical (Detwiler et al., 2001). However, none of the phenotypes described after disruption of these genes in *C. elegans* approximates the two-cell arrest of embryonic development of the ΔN-Zfp36l2 mouse. Because the phenotype we describe is only seen when the *ΔN-Zfp36l2* mutation originates with the females, our findings implicate *Zfp36l2* as a potential maternal effect gene. Whether this phenotype is secondary to the continued presence of specific mRNAs that fail to be degraded by ΔN-Zfp36l2, possibly resulting in elevated levels of maternal proteins derived from these mRNAs, remains to be determined.

Our results strongly suggest that the amino-terminus of Zfp36l2 plays a critical biochemical role in early embryonic development, raising the intriguing possibility that this sequence contains a potential functional domain. Because the two previously characterized domains of Zfp36l2, the tandem zinc finger RNA-binding domain (Lai et al., 2000) and the carboxyl-terminal nuclear export sequence (Phillips et al., 2002) are still present, it is possible that the amino-terminus of Zfp36l2 is involved in regulating the interaction of the protein with other cellular proteins or structures. This putative interaction might therefore represent an attractive target for novel contraceptive strategies. The Zfp36l2 amino-terminus contains a leucine-rich region that resembles a leucine-rich repeat present in the *Mater* gene product (Tong et al., 2000), which, like Zfp36l2, is required for the progression of mouse embryos beyond the two-cell stage.

By analogy with the mouse model, Zfp36l2 may also be involved in the regulation of early embryonic development in humans. Abnormalities in its expression or structure could be involved in some proportion of the 10% of cases of human female infertility that are still without a known cause (Greenhouse et al., 1998). Recent resequencing of the gene encoding human *ZFP36l2* in 72 humans from diverse ethnic groups did not identify any gross splicing mutations that might lead to amino terminal truncation of ZFP36l2 in humans (Blackshear et al., 2003). Nonetheless, 9/23 human ESTs in GenBank on 11/20/03 that spanned the single intron splice site contained retained intronic sequences, and the mRNAs from which they were derived would probably encode the truncated protein. Future resequencing studies will therefore focus on women with unexplained primary infertility.

We are grateful to Lutz Birnbaumer, Ken Korach and Mitch Eddy for helpful comments on the manuscript, to Bob Maronpot and Barbara Davis for discussion of the histological sections, to James Clark and Meilang Flowers for technical assistance, and to Jeff Reece for assistance with confocal microscopy. S.B.V.R. is on leave of absence from the Health Department – Prefeitura Municipal da cidade de Ribeirão Preto, São Paulo, Brazil.

References

Bachvarova, R. and De Leon, V. (1980). Polyadenylated RNA of mouse ova and loss of maternal RNA in early development. *Dev. Biol.* **74**, 1-8.

Blackshear, P. J. (2002). Tristetraprolin (TTP) and other CCCH tandem zinc finger proteins in the regulation of mRNA turnover. *Biochem. Soc. Trans.* **30**, 945-952.

Blackshear, P. J., Phillips, R. S., Vazquez-Matias, J. and Mohrenweiser, H. (2003). Polymorphisms in the genes encoding members of the tristetraprolin family of human tandem CCCH zinc finger proteins. *Prog. Nucleic Acids Res. Mol. Biol.* **75**, 43-68.

Brinster, R. L., Chen, H. Y., Trumbauer, M. E., Yagle, M. K. and Palmiter, R. D. (1985). Factors affecting the efficiency of introducing foreign DNA into mice by microinjecting eggs. *Proc. Natl. Acad. Sci. USA* **82**, 4438-4442.

Burns, K. H., Viveiros, M. M., Ren, Y., Wang, P., DeMayo, F. J., Frail, D. E., Eppig, J. J. and Matzuk, M. M. (2003). Roles of NPM2 in chromatin and nuclear organization in oocytes and embryos. *Science* **300**, 633-636.

Carballo, E., Gilkeson, G. S. and Blackshear, P. J. (1997). Bone marrow transplantation reproduces the tristetraprolin-deficiency syndrome in recombination activating gene-2 (–/–) mice. Evidence that monocyte/macrophage progenitors may be responsible for TNF-alpha overproduction. *J. Clin. Invest.* **100**, 986-995.

Carballo, E., Lai, W. S. and Blackshear, P. J. (1998). Feedback inhibition of macrophage tumor necrosis factor-alpha production by tristetraprolin. *Science* **281**, 1001-1004.

Christians, E., Davis, A. A., Thomas, S. D. and Benjamin, I. J. (2000). Maternal effect of Hsf1 on reproductive success. *Nature* **407**, 693-694.

Clegg, K. B. and Pikó, L. (1983). Poly(A) length, cytoplasmic adenylation and synthesis of poly(A)+ RNA in early mouse embryos. *Dev. Biol.* **95**, 331-341.

DeRenzo, E., Reese, K. J. and Seydoux, G. (2003). Exclusion of germ plasma proteins from somatic lineages by cullin-dependent degradation. *Nature* **424**, 685-689.

Detwiler, M. R., Reuben, M., Li, X., Rogers, E. and Lin, R. (2001). Two zinc finger proteins, OMA-1 and OMA-2, are redundantly required for oocyte maturation in *C. elegans*. *Dev. Cell* **1**, 187-199.

Fraser, L. R. and Drury, L. (1975). The relationship between sperm concentration and fertilization in vitro of mouse eggs. *Biol. Reprod.* **13**, 513-518.

Greenhouse, S., Rankin, T. and Dean, J. (1998). Genetic causes of female infertility: targeted mutagenesis in mice. *Am. J. Hum. Genet.* **62**, 1282-1287.

Gomperts, M., Pascall, J. C. and Brown, K. D. (1990). The nucleotide sequence of a cDNA encoding an EGF-inducible gene indicates the existence of a new family of mitogen-induced genes. *Oncogene* **5**, 1081-1083.

Guedes, S. and Priess, J. R. (1997). The *C. elegans* MEX-1 protein is present in germline blastomers and is a P granule component. *Development* **124**, 731-739.

Jones, E. C. and Krohn, P. L. (1960). Orthotopic ovarian transplantation in mice. *J. Endocrinol.* **20**, 135-146.

Koller, B. H. and Smithies, O. (1989). Inactivating the beta 2-microglobulin locus in mouse embryonic stem cells by homologous recombination. *Proc. Natl. Acad. Sci. USA* **86**, 8932-8935.

Lai, W. S., Stumpo, D. J. and Blackshear, P. J. (1990). Rapid insulin-stimulated accumulation of an mRNA encoding a proline-rich protein. *J. Biol. Chem.* **265**, 16556-16563.

Lai, W. S., Carballo, E., Strum, J. R., Kennington, E. A., Phillips, R. S. and Blackshear, P. J. (1999). Evidence that tristetraprolin binds to AU-rich elements and promotes the deadenylation and destabilization of tumor necrosis factor alpha mRNA. *Mol. Cell. Biol.* **19**, 4311-4323.

Lai, W. S., Carballo, E., Thorn, J. M., Kennington, E. A. and Blackshear, P. J. (2000). Interactions of CCCH zinc finger proteins with mRNA. Binding of tristetraprolin-related zinc finger proteins to AU-rich elements and destabilization of mRNA. *J. Biol. Chem.* **275**, 17827-17837.

Lai, W. S., Kennington, E. A. and Blackshear, P. J. (2003). Tristetraprolin and its family members can promote the cell-free deadenylation of AU-rich element-containing mRNAs by the poly(A) ribonuclease. *Mol. Cell. Biol.* **23**, 3798-3812.

Lin, R. (2003). A gain-of-function mutation in *oma-1*, a *C. elegans* gene required for oocyte maturation, results in delayed degradation of maternal proteins and embryonic lethality. *Dev. Biol.* **258**, 226-239.

Liu, C., Litscher, E. S., Mortillo, S., Sakai, Y., Kinloch, R. A., Stewart, C. L. and Wassarman, P. M. (1996). Targeted disruption of the mZP3 gene results in production of eggs lacking a zona pellucida and infertility in female mice. *Proc. Natl. Acad. Sci. USA* **93**, 5431-5436.

Martin, G. R. (1981). Isolation of a pluripotent cell line from early mouse embryos cultured in medium conditioned by teratocarcinoma stem cells. *Proc. Natl. Acad. Sci. USA* **78**, 7634-7638.

Matzuk, M. M. and Lamb, D. J. (2002). Genetic dissection of

mammalian fertility pathways. *Nat. Cell Biol. Nat. Med.* s41-s49. (www.nature.com/fertility).

Mello, C. C., Schubert C., Draper, B., Zhang, W., Lobel, R. and Preiss, J. R. (1996). The PIE-1 protein and germline specification in *C. elegans* embryos. *Nature* **382**, 710-712.

Perreault, S. D. and Mattson, B. A. (1993). Morphological evaluation of oocytes. In *Methods in Toxicology Vol. 3B: Female Reproductive Toxicology* (ed. J. J. Heindel and R. E. Chapin), pp. 110-127. San Diego, CA: Academic Press.

Phillips, R. S., Ramos, S. B. V. and Blackshear, P. J. (2002). Members of the tristetraprolin family of tandem CCCH zinc finger proteins exhibit CRM1-dependent nucleocytoplasmic shuttling. *J. Biol. Chem.* **277**, 11606-11613.

Rankin, T., Familari, M., Lee, E., Ginsberg, A. M., Dwyer, N., Blanchette-Mackie, J., Drago, J., Westphal, H. and Dean, J. (1996). Mice homozygous for an insertional mutation in the Zp3 gene lack zona pellucida and are infertile. *Development* **122**, 2903-2910.

Schubert, C. M., Lin, R., de Vries, C. J., Plasterk, R. H. and Priess, J. R. (2000). MEX-5 and MEX-6 function to establish soma/germline asymmetry in early *C. elegans* embryos. *Mol. Cell* **5**, 671-682.

Schultz, R. M. (1993). Regulation of zygotic gene activation in the mouse. *BioEssays* **15**, 531-538.

Stumpo, D. J., Graff, J. M., Albert, K. A., Greengard, P. and Blackshear, P. J. (1989). Molecular cloning, characterization, and expression of a cDNA encoding the '80- to 87-kDa' myristoylated alanine-rich C kinase substrate: a major cellular substrate for protein kinase C. *Proc. Natl. Acad. Sci. USA* **86**, 4012-4016.

Stumpo, D. J., Byrd, N. A., Phillips, R. S., Ghosh, S., Maronpot, R. R., Castranio, T., Byrd, N., Meyers, E. N., Mishina, Y. and Blackshear, P. J. (2004). Chorioallantoic fusion defects and embryonic lethality resulting from disruption of *Zfp36L1*, a gene encoding a CCCH tandem zinc finger protein of the tristetraprolin family. *Mol. Cell. Biol.* **24**, 6445-6455.

Tabara, H., Hill, R. J., Mello, C. C., Priess, J. R. and Kohara, Y. (1999). pos-1 encodes a cytoplasmic zinc-finger protein essential for germline specification in *C. elegans*. *Development* **126**, 1-11.

Taylor, G. A., Carballo, E., Lee, D. M., Lai, W. S., Thompson, M. J., Patel, D. D., Schenkman, I. G., Gilkeson, G. S., Broxmeyer, H. E., Haynes, B. F. et al. (1996). A pathogenetic role for TNF alpha in the syndrome of cachexia, arthritis, and autoimmunity resulting from tristetraprolin (TTP) deficiency. *Immunity* **4**, 445-454.

Tong, Z.-B., Gold, L., Pfeifer, K. E., Dorward, H., Lee, E., Bondy, C. A., Dean, J. and Nelson, L. M. (2000). Mater, a maternal effect gene required for early embryonic development in mice. *Nat. Genet.* **26**, 267-268.

Varnum B. C., Ma Q., Chi, T., Fletcher, B. and Herschman, H. R. (1991). The TIS11 primary response gene is a member of a gene family that encodes proteins with highly conserved sequence containing an unusual cys-his repeats. *Mol. Cell. Biol.* **11**, 1754-1758.

Wormington M. (1994). Unmasking the role of the 3′ UTR in the cytoplasmic polyadenylation and translational regulation of maternal mRNAs. *BioEssays* **16**, 533-535.

Wu, X., Viveiros, M. M., Eppig, J. J., Bai, Y., Fitzpatrick, S. L. and Matzuk, M. M. (2003). Zygote arrest 1 (*Zar1*) is a novel maternal-effect gene critical for the oocyte-to-embryo transition. *Nat. Genet.* **33**, 187-191.